Interspecies interactions determine growth dynamics of biopolymer-degrading populations in microbial communities

Journal Article

Author(s):
D'Souza, Glen; Schwartzman, Julia; Keegstra, Johannes (iD); Schreier, Jeremy E.; Daniels, Michael; Cordero, Otto X.; Stocker, Roman; Ackermann, Martin
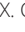
Interspecies interactions determine growth dynamics of biopolymer-degrading populations in microbial communities

Glen D'Souza[a,b,1] (ID), Julia Schwartzman[c,2] (ID), Johannes Keegstra[d] (ID), Jeremy E. Schreier[e] (ID), Michael Daniels[a,b], Otto X. Cordero[c] (ID), Roman Stocker[d] (ID), and Martin Ackermann[a,b,f]

Microbial communities perform essential ecosystem functions such as the remineralization of organic carbon that exists as biopolymers. The first step in mineralization is performed by biopolymer degraders, which harbor enzymes that can break down polymers into constituent oligo- or monomeric forms. The released nutrients not only allow degraders to grow, but also promote growth of cells that either consume the degradation products, i.e., exploiters, or consume metabolites released by the degraders or exploiters, i.e., scavengers. It is currently not clear how such remineralizing communities assemble at the microscale—how interactions between the different guilds influence their growth and spatial distribution, and hence the development and dynamics of the community. Here, we address this knowledge gap by studying marine microbial communities that grow on the abundant marine biopolymer alginate. We used batch growth assays and microfluidics coupled to time-lapse microscopy to quantitatively investigate growth and spatial distribution of single cells. We found that the presence of exploiters or scavengers alters the spatial distribution of degrader cells. In general, exploiters and scavengers—which we collectively refer to as cross-feeder cells—slowed down the growth of degrader cells. In addition, coexistence with cross-feeders altered the production of the extracellular enzymes that break down polymers by degrader cells. Our findings reveal that ecological interactions by nondegrading community members have a profound impact on the functions of microbial communities that remineralize carbon biopolymers in nature.

cross-feeding | community assembly | spatial organization | biopolymer degradation | dispersal

Heterotrophic microbial communities drive the remineralization of carbon, which predominantly exists as biopolymers like chitin (1), alginate (2), cellulose (3), and xylan (4) in natural ecosystems, and thus drive a central step in the biogeochemical cycling of carbon (5–7). Within these communities, multiple microbial guilds coexist and engage in metabolic interactions. A key challenge of microbial ecology is to understand how these metabolic interactions influence the rate of carbon remineralization, which is an ecosystem function of major interest (8–11). The assembly of these communities follows intuitive rules (1). The first step in remineralization is carried out by specialized degraders that express hydrolytic enzymes that degrade biopolymers. These hydrolytic enzymes can be associated to the cell-surface, where polysaccharides are degraded with minimal or no loss of hydrolysis products to the extracellular environment, or released into the extracellular environment. Generally, the secretion of these enzymes leads to the formation of breakdown products. These products support the growth of the degraders and are also released into the environment, alongside with metabolites released by the growing degraders. The release of these metabolites creates niches for the growth of cross-feeder taxa that lack the ability to produce biopolymer-degrading enzymes but can utilize breakdown products (i.e., "exploiters") or utilize other metabolites released from degraders and exploiters [i.e., "scavengers"; (9, 10, 12, 13)]. Since degrader cells are positioned at the beginning of these food chains, their growth influences the assembly of downstream cross-feeders in biopolymer-degrading communities (1, 10, 13). Therefore, any ecological interaction that impacts the growth of degrader cells is expected to impact the rate of carbon remineralization but the magnitude of these impacts is currently unknown.

Degrader cells often aggregate while growing on polysaccharides like chitin (14), alginate (15–17), or xylan (4, 18). Previous experimental and computational studies have established that aggregation, by increasing local cell density, allows degrader cells to benefit from the polysaccharide breakdown activities of neighboring cells (4, 15, 19). However, it is generally unclear how growth and collective behaviors of degraders are influenced by the coexistence with cross-feeding species. Since biopolymer breakdown and metabolic byproduct release at the microscale are a consequence of the activities of degraders, it is

Significance

Microbial communities remineralize biopolymers, which dominate the Earth's stock of organic carbon. Degrader species in these communities produce enzymes that break down biopolymers, releasing metabolic products that enable growth of nondegrading species through cross-feeding. While it is clear that degraders drive the assembly of microbial food-webs, it is not known how cross-feeding shapes the behavior and growth of degrader taxa. Using simple marine microbial communities, here we show that the presence of cross-feeders alters the microscale spatial distribution of degrader cells, influencing their growth and degradation activities. Our work reveals an additional layer of complexity in the interactions that shape microbial food-webs, laying a foundation for better understanding how microorganisms drive carbon remineralization, a central process in the carbon cycle.

[1]To whom correspondence may be addressed. Email: glengeralddsouza@gmail.com.

[2]Present address: Department of Biology, University of Southern California, Los Angeles, CA 90089.

important to investigate the impacts of cross-feeding at the microscale on degrader taxa, in order to develop a better understanding on how interactions impact the growth of biopolymer-degrading taxa and ultimately the rate of remineralization.

Here, we sought to address these knowledge gaps using simple two-species microbial communities that degrade alginate, an abundant biopolymer in marine ecosystems, on which the individual behavior of degraders is well characterized (20). We used a combination of batch growth assays and microfluidics coupled to time-lapse microscopy along with spatial analyses in order to quantitatively determine growth and aggregation behaviors of degrader cells when coexisting with cross-feeder cells. We find that the presence of cross-feeder cells influences the growth of degrader cells, indicating that the activity of cross-feeders can substantially alter the function of microbial communities.

Results and Discussion

Growth of Communities Composed of Degrader and Cross-Feeder Populations. As a first step, we measured the growth on alginate of three marine bacterial strains: i) *Vibrio cyclitrophicus* ZF270, ii) *Vibrio tasmaniensis* 1F187, and iii) *Ruegeria* sp. A3M17. Our goal was to investigate whether these natural marine isolates can be used to construct simple communities composed of two strains: an alginate degrader and a cross-feeder. Polymeric alginate (henceforth referred to as alginate) is a linear polysaccharide composed of repeating units of l-glucuronic acid and d-mannuronic acid. The genome of *V. cyclitrophicus* ZF270 encodes a number of polysaccharide lyases (PLs) that hydrolyze the 1,4-glycosidic linkages between the two monomers (Fig. 1). These PLs (one copy of PL6 and five copies of PL7) are predicted to be secreted into the external environmental or anchored (based on the presence of signal peptides) on the cell membrane, and degrade alginate to produce a combination of monomeric and oligomeric products (21). The breakdown products enter cells and are further processed by PL15 and PL17 enzymes inside the cell to metabolites that enter central carbon metabolism (2, 17, 21–23). *V. tasmaniensis* 1F187 and *Ruegeria* sp. A3M17 cells lack alginate lyases but have a set of genes that could potentially confer the ability to import and utilize simpler oligo- or monomeric products resulting from alginate degradation (2, 10). In line with these predictions, we found that only ZF270 cells grew on alginate, whereas the cross-feeders 1F187 and A3M17 could not grow on alginate (*SI Appendix*, Fig. S1 *A* and *B*). We then sought to test whether these cross-feeders can grow on breakdown products resulting from alginate degradation by ZF270 cells. For this, we used alginate that was enzymatically hydrolyzed using commercially available alginate lyases. Previously, we found that digested alginate (henceforth d-alginate) produced by the above method had a higher amount of both monomeric and oligomeric products compared to the polymeric version of alginate (21).

Therefore, we grew strains on d-alginate, thus creating a scenario where cross-feeders experienced breakdown products released due to alginate breakdown. We found that 1F187 grew to substantially higher levels on d-alginate compared to alginate, whereas A3M17 did not benefit from the hydrolysis products (*SI Appendix*, Fig. S1 *A* and *B*). These observations suggest that while 1F187 can indeed cross-feed on monomeric and oligomeric products generated by alginate breakdown (*SI Appendix*, Fig. S2), A3M17 cannot cross-feed on breakdown byproducts under the conditions tested despite encoding potential genes for uptake and utilization.

Since A3M17 cells cannot grow on alginate-derived byproducts, we investigated whether other metabolic byproducts released during growth of ZF270 degrader cells can support growth. Many bacteria, including marine polysaccharide degraders, release organic acids such as acetate in the environment when grown on sugars, that can be used by cross-feeding bacteria to grow (1, 13, 24). Therefore, we investigated whether ZF270 cells release acetate in the growth medium. We compared acetate secretion profiles of ZF270 monocultures with cocultures of ZF270 with A3M17 cells. We found that ZF270 cells secreted a significantly higher concentration of acetate when in monoculture than in coculture (*SI Appendix*, Fig. S3). The low acetate levels combined with higher growth in cocultures (*SI Appendix*, Fig. S3) indicate that the A3M17 cells can use acetate and likely other organic acids secreted by ZF270 cells in order to grow in these microbial communities.

Based on these growth results, we constructed simple two-species communities consisting of the degrader ZF270 and either the oligo-saccharide exploiter 1F187 or the byproduct scavenger A3M17 (Fig. 1*A*). We then asked whether the presence of degraders allowed cross-feeders to grow. In addition, this growth assay enabled the quantification of any beneficial or detrimental effects of cross-feeder cells on degrader cells. When we grew degrader and cross-feeder cells in isolation or together on alginate in shaking flasks, we found that both cross-feeding strains 1F187 (Fig. 1*B*) and A3M17 (Fig. 1*C*) had increased growth yields in the presence of the degrader ZF270. The enhanced growth of A3M17 in coculture with degrader cells suggests that these cells likely cross-feed on metabolic byproducts that are secreted by ZF270 in coculture. Degrader cells displayed enhanced growth yields in the presence of 1F187 exploiter cells (Fig. 1*B*) potentially through the removal of byproduct by the cross-feeding cells. In contrast, the growth yield of the degraders was similar in the presence or absence of A3M17 scavenger cells (Fig. 1*C*). These observations indicate that, in addition to benefitting from the presence of degrader cells within communities, certain cross-feeder strains can also enhance the growth of degrader cells.

Cross-Feeders Influence Growth of Degraders through Secreted Compounds in Model Marine Communities. A possible explanation for how cross-feeder cells influence the growth of degrader cells is through the production or consumption of secreted metabolites (11, 13, 24–28). Cross-feeders can decrease the growth of degraders by consuming metabolites that represent nutrients for degraders, thus reducing the availability of these for degraders, or by producing metabolites that inhibit the growth of degraders (28, 29). Conversely, cross-feeders can increase the growth of degraders by utilizing metabolites that inhibit the growth of degrader cells (13, 26) or by producing metabolites that support degrader growth. To understand the effect of compounds secreted by cross-feeders on the growth of degrader cells, we grew cross-feeder cells, harvested the spent media, and grew degraders on this spent-medium. Since cross-feeders do not grow on alginate, we grew them on substrates permissive to cross-feeder growth. Oligomer-exploiting 1F187 cells were grown on d-alginate for 36 h. A3M17 cells, which scavenge byproducts and did not grow on alginate or d-alginate under the conditions tested (*SI Appendix*, Fig. S1), were grown on alginate supplemented with 0.1% marine broth for 36 h. The spent medium in either case was harvested to remove cross-feeder cells and used to monitor growth of degrader cells (Fig. 2 *A* and *B*). The growth of degraders on spent-medium was then compared to the growth of degraders on spent-medium produced by growing degrader cells on cognate fresh medium (Fig. 2 *A* and *B*). By comparing the growth of degraders on the spent medium of cross-feeders vs. the spent medium of degraders, we were able to differentiate effects on the growth of degraders due to compounds released or utilized by cross-feeders from effects due to the consumption of limiting resources by the cross-feeders.
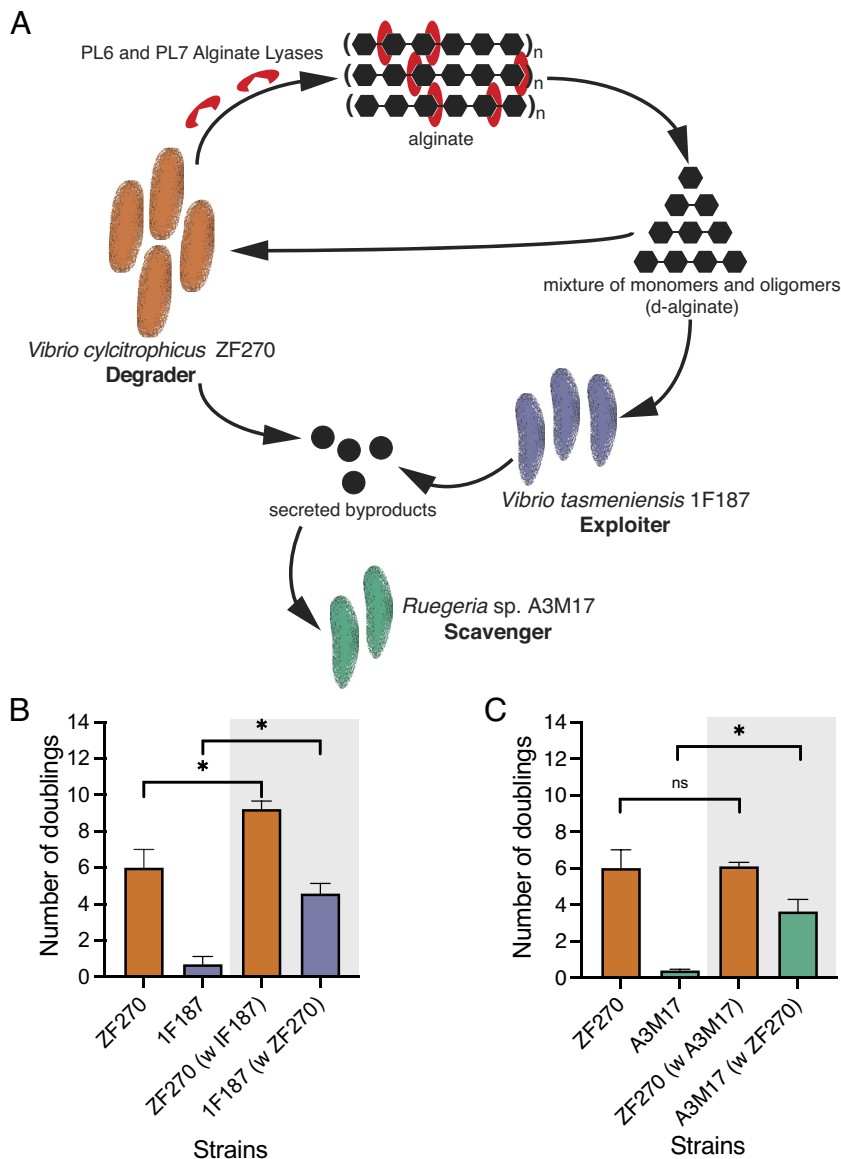
Fig. 1. Growth dynamics of strains within simple two-species microbial communities in well-mixed environments. (*A*) *V. cyclitrophicus* ZF270 cells are predicted to secrete extracellular alginate lyases PL6 and PL7 to degrade the marine polysaccharide alginate, thereby producing a mixture of monomeric and oligomeric breakdown products (2, 17, 21–23). Both *V. tasmaniensis* 1F187 and *Ruegeria* sp. A3M17 cells cannot grow on polymeric alginate (alginate), but 1F187 cells can act as exploiters and grow on degradation products of alginate (d-alginate), while A3M17 can act as a scavenger by feeding on byproducts released from degrader cells (*SI Appendix*, Fig. S1 *A and B*). (*B* and *C*) The cross-feeders can grow in co-culture with the degraders. Growth yield are represented as doublings based on colony counts obtained at the start and end of a 36 h growth cycle (*Materials and Methods*). (*B*) *V. cyclitrophicus* ZF270 and *V. tasmaniensis* 1F187; or (*C*) *V. cyclitrophicus* ZF270 and *Ruegeria* sp. A3M17 in monocultures (no gray shading) or cocultures (gray shading) in shaking flasks with alginate. The bars indicate the mean, whereas the error bars indicate the SD. Asterisks and "ns" indicate statistically significant or nonsignificant comparisons, respectively, among groups (in *B* and *C*: paired *t* tests: ZF270 vs. ZF270 + 1F187: $P = 0.015$, $t = 4.05$, $R^2 = 0.80$, $n_{populations} = 3$; ZF270 vs. ZF270 + A3M17: $P = 0.44$, $t = 0.85$, $R^2 = 0.15$, $n_{populations} = 3$; 1F187 vs. 1F187 + ZF270: $P = 0.013$, $t = 4.25$, $R^2 = 0.81$, $n_{populations} = 3$; A3M17 vs. A3M17 + ZF270: $P = 0.04$, $t = 5.95$, $R^2 = 0.89$, $n_{populations} = 3$).

We found that ZF270 degrader populations reached higher population sizes but showed similar growth rates on spent medium of 1F187 cells (Fig. 2 *C* and *D*) compared to spent medium of ZF270 cells. In contrast, ZF270 degrader populations had both reduced population sizes and growth rates on spent medium of A3M17 cells (Fig. 2 *C* and *D*) compared to spent medium of ZF270 cells. These observations indicate that cross-feeders indeed modify their external environment, through secretion or removal of metabolites and compounds that can positively (1F187) or negatively (A3M17) influence the growth of degrader cells. While the positive influence on ZF270 by 1F187 cells is in line with our earlier observation in cocultures (Fig. 1*B*), the negative influence of A3M17 spent-medium on ZF270 cells (Fig. 2*C*) is a deviation from the neutral effect observed in cocultures (Fig. 1*C*).

Presence of Cross-Feeders Influences Spatial Distribution of Degrader Populations. Since interactions between cross-feeder and degrader cells often manifest at the microscale in natural ecosystems (9, 19, 30), we tested the influence of cross-feeder cells on degrader cells within microfluidic growth devices. These devices are made of an inert polymer—polydimethylsiloxane (PDMS)—bound to a glass coverslip (Fig. 3*A*). Within the PDMS layer are several growth channels. Each of these channels consists of an inlet through which growth medium containing nutrients can be pumped. This medium enters flow channels, (height: 20 μm and width: 100 μm), lateral to which are several growth chambers (Fig. 3*A*). The dimensions of each growth chamber (height: 0.85 μm, length: 60 μm, width: 90 to 120 μm) allow single cells to freely move or adhere to the glass coverslip, which constitutes the floor of
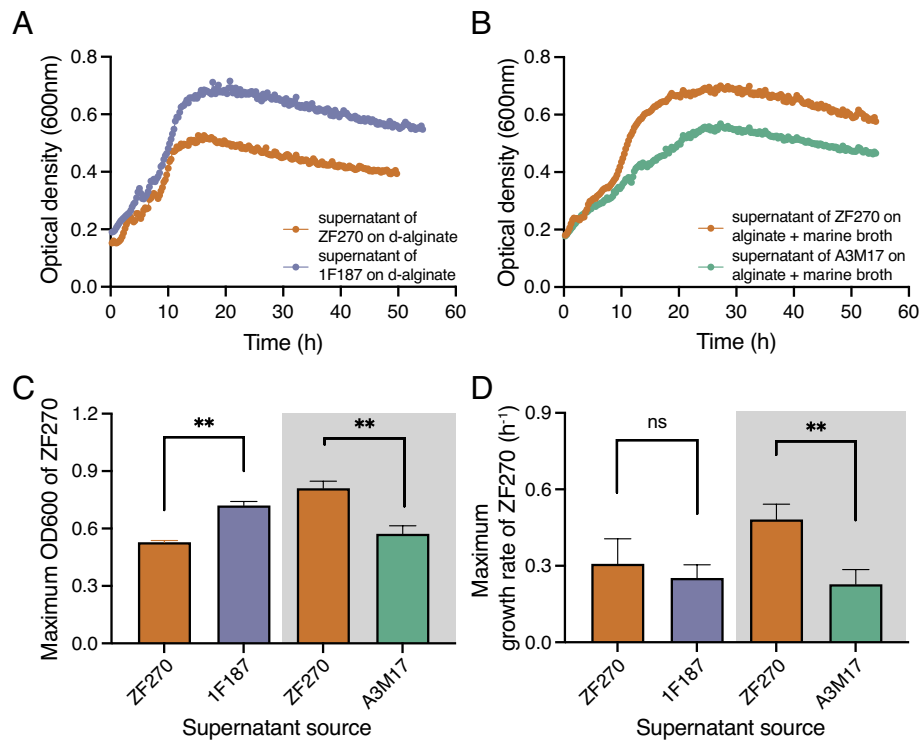
Fig. 2. Spent-medium of cross-feeders alters growth dynamics of *V. cyclitrophicus* ZF270 degrader populations. (*A* and *B*) Growth dynamics (measured as optical density at 600 nm) of *V. cyclitrophicus* ZF270 cells in the presence or absence of spent medium of (*A*) *V. tasmaniensis* 1F187 or (*B*) *Ruegeria* sp. A3M17. (*C*) Maximum population sizes and (*D*) maximum growth rates achieved by *V. cyclitrophicus* ZF270 cells in different spent media (ZF270: orange bars, 1F187: purple bars and A3M17: green bars). Asterisks and "ns" indicate statistically significant and nonsignificant comparisons, respectively, among groups (in *C*: Mann–Whitney test, ZF270 and 1F187: $P < 0.0095$, $n_{populations}$ = 4 to 6; ZF270 + A3M17: $P < 0.0043$, $n_{populations}$ = 5 to 6; in *D*: Mann–Whitney test, ZF270 and 1F187: $P < 0.47$, $n_{populations}$ = 4 to 6; ZF270 + A3M17: $P < 0.0043$, $n_{populations}$ = 5 to 6).

the growth chamber while the PDMS constitutes the ceiling. Cells grow as monolayers because the height of the chamber is less than one micrometer (Fig. 3*A*). The alginate used as carbon source is soluble in the nutrient medium, is constantly pumped through the flow channel and enters the growth chambers, primarily through diffusion (4, 5, 17, 18). Therefore, the number of cells and their positioning within microfluidic chambers are determined by the cellular growth rate as well as by cell movement (18). By combining microfluidics with automated time-lapse microscopy, we imaged the development of communities over time.

ZF270 cells are known to grow as monolayer aggregates when growing on alginate in microfluidic growth chambers (17) and the increased local cell density due to aggregation allows cells to cooperatively degrade alginate. In accordance with previous findings, we found that ZF270 cells form aggregates when growing on alginate (Fig. 3*B*). In the presence of 1F187 cells (Fig. 3*C*), the number of degrader cells within growth chambers was similar to that in monocultures of degraders (*SI Appendix*, Fig. S4*A*). In contrast, the number of degrader cells was reduced when A3M17 cells were present (Fig. 3*D* and *SI Appendix*, Fig. S4*A*). These results indicate that microscale interactions with cross-feeders can impact the growth rate or movement of degrader cells.

In order to quantify the microscale spatial and growth patterns of cells, we analyzed the time-lapse movies using image analysis. Briefly, we performed cell segmentation and tracking and then mapped the lineages of all ZF270 (Fig. 3 *E–G*) and cross-feeder cells present in each growth chamber based on division events. This analysis allowed us to quantify the spatial distribution of cells as well as the rate at which individual cells in a microfluidics growth chamber increase their length and divide.

To understand how the cross-feeders influence the spatial distribution of degrader cells, we quantified the local density of ZF270 cells

in monoculture and cocultures. This measure allows the determination of packing of ZF270 cells in the presence and absence of cross-feeder cells. For every ZF270 cell, we quantified the density at different radial distances (10 μm, 20 μm, 30 μm, 40 μm, and 50 μm) from the focal cell. This analysis revealed that local density decreased as the radial distance increased for ZF270 cells in all conditions (Fig. 3*H*), suggesting that cells are more clustered at smaller scales. However, the level of clustering differs between the three conditions.

When in monoculture, ZF270 had the highest local density across all radii tested (Fig. 3*H*), indicating that most cells are clustered together at all scales and form aggregates. The presence of exploiter 1F187 cells decreases the local density of ZF270 (Fig. 3*H*), suggesting that cells form aggregates but less than what they form in monoculture. In the presence of the scavenger A3M17, ZF270 had the lowest local density (Fig. 3*H*), suggesting that degrader cells are least likely to aggregate in presence of scavengers. In addition to the local density, we also measured the global density (corresponding to the number of cells per area) of ZF270 cells in each growth chamber. This analysis also revealed that ZF270 cells in monoculture have the highest global density compared to ZF270 cells in coculture with 1F187 or ZF270 cells in the presence of A3M17 (*SI Appendix*, Fig. S4*B*), which had the lowest global density of the three conditions. In addition, for degrader ZF270 cells, we quantified the relationship between either the local density (*SI Appendix*, Fig. S4*C*) or global density (*SI Appendix*, Fig. S4*D*) with the number of resident cells in each chamber. This analysis revealed that both local density (*SI Appendix*, Fig. S4*C*) and global density (*SI Appendix*, Fig. S4*D*) increase with the number of cells. However, the increase is steeper for ZF270 monocultures followed by cocultures with 1F187 and cocultures with A3M17 (*SI Appendix*, Fig. S4 *C* and *D*), again indicating that the presence of cross-feeders reduces the aggregative behaviors of ZF270 cells.
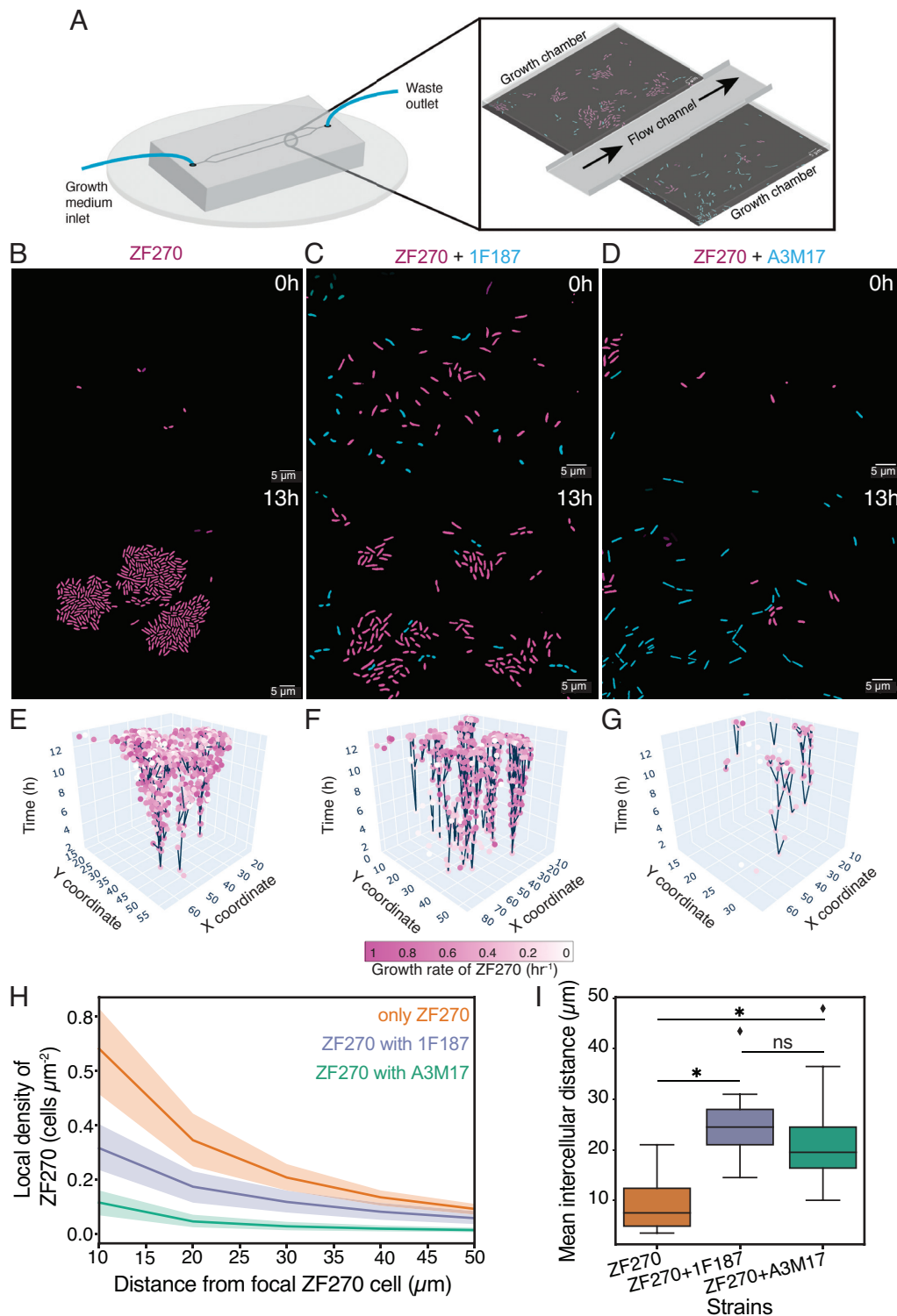
Fig. 3. Aggregate formation by *V. cyclitrophicus* ZF270 populations is influenced by the presence of cross-feeders. (*A*) Overview (top-view) of microfluidic growth device and setup of experiment. Microfluidic devices were made out of PDMS elastomers and were plasma bonded to a glass coverslip. Growth chambers were 90 to 120 × 60 × 0.85 μm and faced a nutrient feeding channel of 22 μm in height and 100-μm wide. Shown are snapshots of cells within microfluidic chambers at a representative time point. (*B–D*) Representative images of microfluidic growth chambers containing (*B*) monocultures of *V. cyclitrophicus* ZF270, (*C*) cocultures of *V. cyclitrophicus* ZF270 with *V. tasmaniensis* 1F187, and (*D*) *V. cyclitrophicus* ZF270 with *Ruegeria* sp. A3M17 cells. The *Upper* panel are representative images of chambers at initiation of growth, i.e., 0 h, whereas the *Lower* panels are images of chamber 13 h after initiation. *V. cyclitrophicus* ZF270 are false colored in magenta, whereas cells of *V. tasmaniensis* 1F187 and *Ruegeria* sp. A3M17 are false colored in cyan. (*E–G*) Lineage trees of ZF270 cells growing (*E*) as monocultures, (*F*) in the presence of 1F187 cells; and (*G*) in the presence of A3M17 cells. Cells (magenta spheres) are plotted as a function of their spatial location (*x* and *y* coordinates) and time (*z* coordinate) within a microfluidic growth chamber. Black segments connect cells that are related through cell division, while branching points mark division events. The color intensity of the magenta spheres indicates the growth rate (h^{-1}) of individual cells. (*H*) Local density of ZF270 cells in monoculture (orange), presence of 1F187 cells (purple), or presence of A3M17 cells (green). Local density (cells μm^{-2}) was computed as the density within distinct radial distances (10, 20, 30, 40, 50) from every focal ZF270 cell. ZF270 cells have a higher local density at all radial distances when in monocultures compared to when ZF270 cells are in the presence of 1F187 and A3M17 cells. Lines are fits of nonlinear polynomial regression models (ZF270: $R^2 = 0.71$, $P < 0.0001$, $Density_{local} = 1.03 + (-0.04*Radius) + 0.0004*Radius^2$; ZF270 with 1F187: $R^2 = 0.56$, $P < 0.0001$, $Density_{local} = 0.46 + (-0.017*Radius) + 0.00018*Radius^2$; ZF270 with A3M17: $R^2 = 0.48$, $P < 0.0001$, $Density_{local} = 0.18 + (-0.008*Radius) + 9.87e-05*Radius^2$). (*I*) Mean intercellular distances between ZF270 cells in monoculture (orange), ZF270 cells and 1F187 cells (purple) or ZF270 cells and A3M17 cells (green) estimated using the pair correlation function (*Materials and Methods*). Box plots extend from the 25th to 75th percentiles and whiskers indicate the 10th and 90th percentiles of mean peak intercellular distances. Differences are statistically nonsignificant (indicated by *ns*), and outliers are indicated as diamonds (Mann–Whitney *U* tests—ZF270-ZF270 and ZF270-1F187: *U* = 68, *P* = 0.002; ZF270-ZF270 and ZF270-A3M17: *U* = 53.5, *P* = 0.02; ZF270-1F187 and ZF270-1F187: *U* = 48.5, *P* = 0.24).

Finally, we also quantified the intercellular distances between ZF270 and cross-feeder cells in either coculture condition. For this, we use the pair correlation function [pcf (paircorrelation function); see *Materials and Methods*], which estimates the probability of finding a cross-feeder cell at different distances from a ZF270 cell, normalized by the average probability if the cells were distributed uniformly. We mapped the pcf for every degrader–degrader and degrader-cross-feeder cell pair in each chamber and

calculated the distance at which peak pcf was attained, a measure we termed the mean intercellular distance (Fig. 3*I* and *SI Appendix*, Fig. S5). This analysis revealed that both cross-feeders were often found at similar intercellular distances (on average 20 to 25 μm) from degrader cells at all time points (Fig. 3*I* and *SI Appendix*, Fig. S5).

In summary, our spatial analysis revealed that cross-feeders are often present at larger distances from degraders, compared to

degrader–degrader pairs (Fig. 3*I*), but their presence alters the spatial distribution of degrader cells. In addition, the detrimental effect of A3M17 scavengers on growth of ZF270 degraders observed in well-mixed experiments (Fig. 2*C*) is in line with the reduction in group sizes (*SI Appendix,* Fig. S4*B*) and altered spatial distribution (Fig. 3*H*) of degraders at the microscale.

Coexistence with Cross-Feeding Cells Shifts the Temporal Growth Dynamics of Degrader Cells. Since the presence of cross-feeders alters the spatial distribution and density of degrader cells, and the growth of degrader cells on polymers depends on increased cell densities (4, 17), we expected interactions with cross-feeders to alter growth dynamics of degraders. To quantify these effects, we measured the single-cell growth rates of ZF270 cells that were grown on alginate in the absence or presence of either cross-feeding cell-type (Fig. 3 *E*–*G*). We then analyzed the distribution of growth rates of single cells that were born at different time points in microfluidic growth chambers. We found that degrader ZF270 cells growing in monoculture achieved their maximum growth rates 8 h after the start of the growth experiment (Fig. 4). However, the presence of either cross-feeder reduced the maximum median growth rate while increasing the time to reach the maximum growth rate of degrader cells. When

oligomer-exploiter 1F187 cells were present, ZF270 cells reached their maximum growth rate after approximately 10 h of growth initiation, whereas scavenger A3M17 cells delayed the time to maximum growth rate of degrader cells to 13 h (Fig. 4).

The detrimental effect of 1F187 on the growth dynamics of the degraders (Fig. 4) was in contrast to the observation in well-mixed environments that spent-medium of 1F187 cells benefited ZF270 cells (Fig. 2 *A* and *C*). Such an observation could arise if 1F187 cells compete with the degrader cells at the microscale for breakdown products resulting from alginate degradation. The findings that byproduct scavenging A3M17 cells reduced density (Fig. 3*H* and *SI Appendix,* Fig. S4) and decreased growth rates (Fig. 4) of ZF270 cells align well with the observations of the spent-medium experiments, further lending credence to the idea that A3M17 cells negatively influence the growth of degrader cells, potentially through secretion or utilization of compounds.

Since the growth of ZF270 cells is dependent on cell density (17), a reduced density in the presence of cross-feeder cells can alter growth rates of degrader cells. Therefore, we analyzed the relationship between global density and growth rate of ZF270 cells in monocultures or communities. This analysis revealed that there is indeed a relationship between density and growth rate (Fig. 4*C*). ZF270 cells growing in the presence of scavenger A3M17 cells
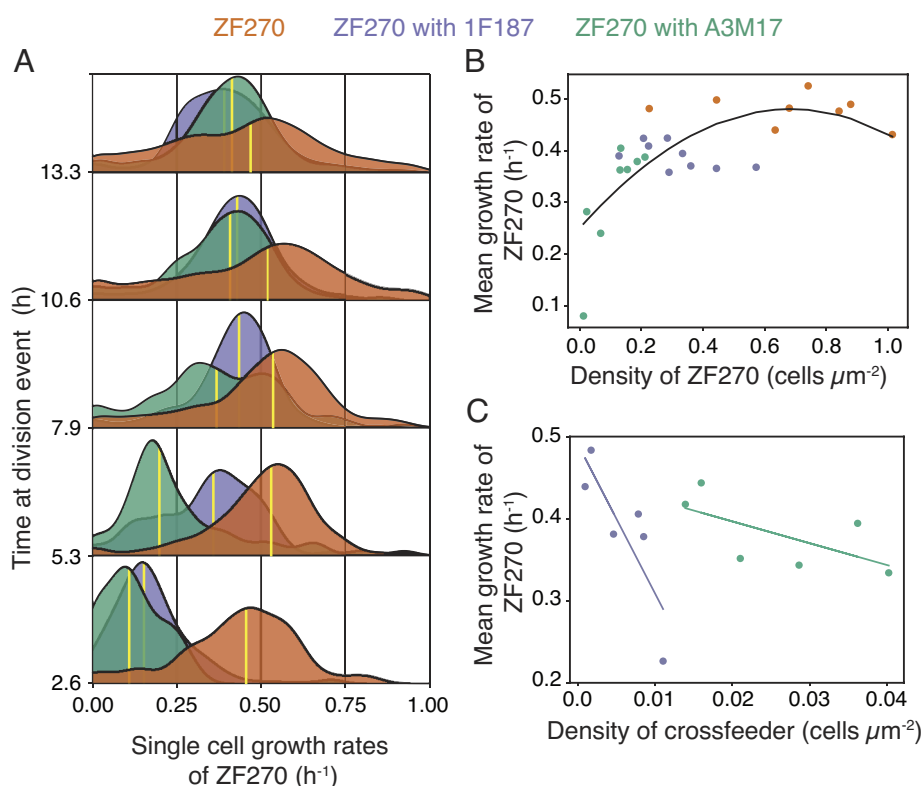

Fig. 4. Presence of cross-feeder cells shifts the temporal growth dynamics of degrader cells. (*A*) Single-cell growth rates of all *V. cyclitrophicus* ZF270 cells growing in microfluidic growth chambers were measured in monocultures (orange) or in cocultures with *V. tasmaniensis* 1F187 (purple) and *Ruegeria* sp. A3M17 (green) cells. Growth rates of cells were binned into time intervals based on the time they emerged from division. ZF270 cells growing in monoculture reach maximal growth rates faster than *V. cyclitrophicus* ZF270 cells growing along with *V. tasmaniensis* 1F187 and *Ruegeria* sp. A3M17. The distributions are pooled for all replicates. Cells were binned into 2.65-h intervals based on the time at a division event (bins: 0 to 2.65 h, 2.66 to 5.30 h, 5.31 to 7.9 h, 7.91 to 10.60 h, and 10.61 to 13.4 h). Yellow horizontal lines depict the medians of the distributions (n_{cells} of ZF270: monocultures = 10,585, with 1F187 = 7,698, with A3M17 = 1,485). Medians of individual chambers are statistically significantly different. (One-way ANOVA - 2.6 h: $R^2 = 0.95$, $P < 0.0001$, $F = 212.7$; 5.3 h: $R^2 = 0.76$, $P < 0.0001$, $F = 35.25$; 7.9 h: $R^2 = 0.42$, $P = 0.0025$, $F = 7.99$). (*B*) Mean growth rate (h^{-1}) of ZF270 cells as function of global cell density (*SI Appendix,* Fig. S4*B*) in microfluidic growth chambers. Each circle represents mean growth dynamics and density of ZF270 cells in one of the three conditions. The relationship follows a polynomial growth model (Model: Growth rate = $-0.49x^2 + 0.67x + 0.25$, where x is cell number; rmse: 0.06, $R^2 = 0.54$; Pearson correlation = 0.62, $P = 0.0009$) indicated by the black curve (based on best fits, see *SI Appendix,* Table S1 for details on fits for linear and nonlinear regression models). (*C*) Correlation between final growth rate (h^{-1}) of ZF270 cells and density of cross-feeder cells in microfluidic growth chambers. The correlation tends to be more negative for ZF270 cells in coculture with 1F187 cells (rmse: 0.04, $R^2 = 0.70$; Pearson correlation = -0.84, $P = 0.038$) compared to ZF270 cells in coculture with A3M17 cells (rmse: 0.03, $R^2 = 0.42$; Pearson correlation = -0.64, $P = 0.167$)

have the lowest densities and thus lowest growth rates (Fig. 4*C*), while degraders growing in the presence of exploiter 1F187 cells have comparatively higher densities and as a result have a higher growth rate as well (Fig. 4*C*). The ZF270 cells in monoculture have the highest density as well as growth rates compared to ZF270 cells growing along with cross-feeder cells (Fig. 4*C*).

We also investigated whether the density of cross-feeder cells had any effect on the growth rates of degrader cells for all microfluidic growth chambers where degrader and cross-feeder cells were present at the end of the experiment. We found that the growth rate of ZF270 cells tends to have a negative relationship with the density of cross-feeder cells (Fig. 4*D*). ZF270 cells that are present along with exploiter cells have an increased reduction in growth rate with increases in density of the cross-feeder (Fig. 4*D*) compared to ZF270 cells growing in the presence of scavenger cells. When the growth rate of cross-feeders was analyzed, the byproduct scavenging A3M17 achieved higher growth rates compared to the oligomer-exploiter 1F187 (at 7.9 h, *SI Appendix*, Fig. S6). Taken together, our results suggest that the presence of cross-feeders alters growth dynamics of degrader cells likely due to an altered spatial distribution of degrader cells at the microscale.

Cross-Feeder Cells Alter Activity and Secretion of Polysaccharide-Degrading Enzymes by Degraders. Since the presence of cross-feeders alters the growth dynamics of degrader cells, it is plausible that the activity of alginate lyases, enzymes that mediate breakdown of alginate, is also altered. In ZF270 cells, alginate lyases are secreted extracellularly (17, 21). Therefore, quantifying the activity of alginate lyases enabled the measurement of the effect of cross-feeders on the enzyme activity of degraders. For this, we used a plate-based assay where ZF270 monocultures or cocultures were spotted on alginate plates along with one of the cross-feeders. In this assay, alginate reacts with iodine to produce a violet compound. The breakdown of alginate by secreted enzymes that diffuse away from the cells creates simpler oligomers or monomers that yield colorless halos when stained with iodine. We measured the diameter of the halo as a proxy for understanding activity of ZF270 cells in the absence or presence of degraders (*SI Appendix*, Fig. S7A

Since the presence of cross-feeders alters the growth dynamics of degrader cells, it is plausible that the activity of alginate lyases, enzymes that mediate breakdown of alginate, is also altered. In ZF270 cells, alginate lyases are secreted extracellularly (17, 21). Therefore, quantifying the activity of alginate lyases enabled the measurement of the effect of cross-feeders on the enzyme activity of degraders. For this, we used a plate-based assay where ZF270 monocultures or cocultures were spotted on alginate plates along with one of the cross-feeders. In this assay, alginate reacts with iodine to produce a violet compound. The breakdown of alginate by secreted enzymes that diffuse away from the cells creates simpler oligomers or monomers that yield colorless halos when stained with iodine. We measured the diameter of the halo as a proxy for understanding activity of ZF270 cells in the absence or presence of degraders (*SI Appendix*, Fig. S7A).

We found that ZF270 populations in coculture with scavenger cells had reduced lyase activity compared to degrader cells in monocultures or ZF270 populations in coculture with exploiter cells (*SI Appendix*, Fig. S7A). The decrease in enzyme activity can be a result of a reduction in the number of cells in the coculture or decreased enzyme secretion per degrader cell. To investigate the reason for the changes in activity, we measured the number of degrader cells in the spotted cultures. We found that the number of ZF270 cells was lower when growing along with scavengers compared to monocultures or cocultures with exploiters (*SI Appendix*, Fig. S7B). When halo sizes were normalized with the cell numbers, the per-cell

alginate lyase activity was higher for ZF270 cells when in coculture with A3M17 compared to ZF270 cells in monocultures or ZF270 cells in coculture in 1F187 (Fig. 5). Similar observations have been made in the case of increased expression of polysaccharide-degrading enzymes of degraders when present along with cross-feeding cells that consume organic acids. (24, 31, 32). We speculate that organic acid secretion by ZF270 cells combined with some form of a yet-to-be-identified cue from A3M17 cells has a role in changes of alginate lyase secretion by ZF270 cells in cocultures with A3M17 cells. Taken together, our findings indicate that in addition to benefitting from the metabolic activities of degrader cells, cross-feeder cells can alter secretion and activity of polysaccharide-degrading enzymes by degrader cells.

Our findings indicate that cross-feeding, which is a prevalent phenomenon in natural microbial communities (11), influences the spatial organization and growth of species that remineralize carbon biopolymers. It is known that biopolymer-degrading bacteria can alter their surface association in response to changes in environmental nutrient composition (4, 23, 33). Our findings indicate that differences in collective behaviors including the spatial distribution of cells can also arise as a consequence of species interactions. These observations suggest that degraders not only structure microbial food-chains but their activity is also shaped by downstream cross-feeding species.

Microorganisms with polysaccharide remineralizing capabilities are prevalent in natural ecosystems and not only impact biogeochemical cycles but are also used as probiotics that facilitate glycan utilization in the context of animal agriculture (3) or for bioremediation of complex polysaccharides (34). These species are usually selected by studying degradation abilities of species in monoculture experiments. In addition, growth dynamics and behaviors such as aggregation or dispersal are usually studied in clonal populations. Our findings reveal the importance of understanding such behaviors in the context of a multispecies community because members downstream of the actual degradation influence growth of degrading strains. In addition, our study demonstrates that the type of cross-feeding interaction determines the impact on growth of taxa that form the base of polysaccharide-degrading food webs.

While our findings are based on studying simple communities composed of natural marine isolates growing on the polysaccharide
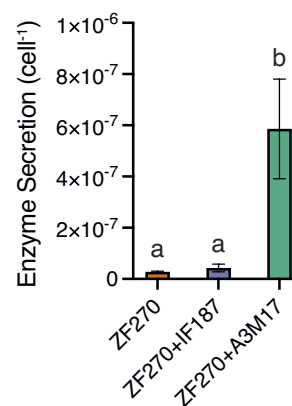

Fig. 5. Crossfeeders alter enzyme secretions by degrader cells. (*A*) Alginate lyase enzyme secretion per degrader cell is higher for *V. cyclitrophicus* ZF270 populations growing together with *Ruegeria* sp. A3M17 cells (green) compared to ZF270 cells growing in monoculture (orange) or ZF270 cells growing together with *V. tasmaniensis* 1F187 cells (purple). Per-cell enzyme secretions were calculated by dividing the halo diameters (*SI Appendix*, Fig. S7A) measured using an iodine assay after a 36-h growth cycle (*Materials and Methods*) with cell numbers measured using plating (*SI Appendix*, Fig. S7B). The bars represent the mean (n = 3) while error bars indicate the SD. Letters *A* and *B* indicate statistically distinct groups based on significant differences between comparisons (one-way ANOVA and Dunnett's multiple comparison test, F = 23.97, P = 0.0014, R^2 = 0.88).

alginate, similar observations have been made for chitin degrading soil microbial communities, where it has been shown that the phenotype of a species, with regard to its role as a degrader, is driven by the constituent members of the community (35). In addition, it is known that the anaerobic remineralization of many organic compounds to methane by bacteria only proceeds if the degradation end products are maintained at low levels due to consumption by syntrophic bacteria, that often exist in close spatial proximities of degraders (36, 37). Similarly cross-feeders in dental plaque communities can stimulate the expression of polysaccharide-degrading enzymes in degrader cells causing degraders to breakdown starch and release organic acids that can be utilized by cross-feeder cells (32). Therefore, these findings highlight the necessity of taking into account ecological interactions in addition to in silico predictions of ecosystem function based on the enzymatic functions encoded within metagenomes (38). Although natural communities often have a large and diverse set of species in comparison with the simple communities used in our experiments, they still consist of few functional groups: degraders, exploiters, and scavengers (10, 12). Therefore, our findings can be applied to explain microscale interactions and successional patterns in microbial communities. However, an important caveat to note is that species within natural communities have access to multiple polysaccharides at the same time, that can alter interaction networks and functions of species.

Ultimately, our results underscore the importance of understanding behaviors at the level of single cells (39) and investigating how individuals within communities react to the presence of cells belonging to different species. Uncovering the molecular mechanisms that underlie behavioral responses will enable a stronger understanding of not only the drivers of community assembly and spatial organization within communities but also allow the development of potential applications to systematically control the composition and behavior of microbial ecosystems (40).

Materials and Methods

Bacterial Strains, Media, and Growth Assays. We used *V. cyclitrophicus* ZF270, *V. tasmaniensis* 1F187, and *Ruegeria* sp. A3M17 that contained plasmids bearing fluorescent proteins: ZF270–pLL103-mKate2, 1F187–pLL102-mCitrine, and A3M17-pJES005-mCit (*SI Appendix*, Table S2). Strains are freely available on request and will also be available from the Culture Collection of Switzerland.

Strains were cultured in Marine Broth (DIFCO) and grown for 18 h at 25 °C. Cells from these cultures were used for growth experiments in Tibbles Rawling (TR) minimal medium (40) containing either 0.1% (weight/volume) Polymeric alginate (Sigma Aldrich) or 0.1% degraded (d) alginate. D-alginate was produced by enzymatically degrading 2% alginate with 1 unit mL^{-1} of alginate lyase (Sigma Aldrich) at 37 °C for 24 h. Then, 100 mL of this mixture was generated, and the breakdown products have been measured previously with high-performance liquid chromatography to show that d-alginate contains a significantly higher amount of monomeric and oligomeric breakdown products of alginate than polymeric alginate (21). Carbon sources were prepared in nanopure water and filter sterilized using 0.40-μm Surfactant-Free Cellulose Acetate filters (Corning, USA). Well-mixed batch experiments in alginate or d-alginate media were performed in 96-well plates, and growth dynamics were measured using a micro-well plate reader (Biotek, USA).

Growth Assays. Coculture assays were initiated as described previously (41). To measure growth of degrader and cross-feeding strains in communities, ~10^5 colony-forming units (CFUs) mL^{-1} of either strain were inoculated into 10 mL TR medium with the requisite carbon source, and cell numbers were determined at 0 h and 36 h by plating. Strains display distinct morphologies and harbor different fluorescent phenotypic markers and therefore can be differentiated on Marine Agar [Marine broth with 1.5% Agar (Applichem) plates. Growth of strains was determined by calculating the number of doublings of individual strains in mono- or co-cultures: Doublings = ($\log_2 (N_f/N_i)$], where N_i is the initial number of CFUs at 0 h and N_f is the final CFU count (41, 42).

Spent-Medium Experiments. To generate spent medium of degraders, *V. cyclitrophicus* ZF270 cells (~10^5 CFUs mL^{-1}) were grown in 10 mL TR medium with 0.1% alginate for 36 h. Cells were separated from the supernatant by centrifugation at 10,000 rpm for 10 min followed by filtering through 0.40-μm Surfactant-Free Cellulose Acetate filters (Corning, USA). The supernatants were then used to grow cross-feeder populations, whose growth was initiated at starting densities of ~10^5 CFUs mL^{-1}. To generate supernatants of *V. tasmaniensis* 1F187, cells (~10^5 CFUs mL^{-1}) were first grown on 0.1% d-alginate TR medium for 36 h following which supernatants were harvested as described above. Growth of *V. cyclitrophicus* ZF270 cells was then initiated at ~10^5 CFUs mL^{-1} on supernatant as well as on supernatant of d-alginate TR medium where ZF270 cells were grown as a control. To generate supernatants of *Ruegeria* sp. A3M17, cells (~10^5 CFUs mL^{-1}) were grown on MB medium with 0.1% alginate and supernatants harvested as described above. Growth of *V. cyclitrophicus* ZF270 cells was then initiated at ~10^5 CFUs mL^{-1} on supernatant as well as on supernatant of MB medium with 0.1% alginate where ZF270 cells were grown as a control.

Microfluidics and Time-Lapse Microscopy. Microfluidics experiments and microscopy were performed as described previously (4, 5, 43). Cell growth and behavior was imaged within chambers which ranged from 60 to 120 × 60 × 0.85 μm. ($l × b × h$) Within these chambers, cells attach to the glass surface and experience the medium that diffused through the lateral flow channels. Imaging was performed using IX83 inverted microscope systems (Olympus, Japan) with automated stage controller (Marzhauser Wetzlar, Germany), shutter, and laser-based autofocus system (Olympus ZDC 2). Chambers were imaged in parallel on the same PDMS chip, and phase-contrast and fluorescent (mKate2 and/or mCitrine) images of each position were taken every 8 or 10 min. The microscopy unit and PDMS chip was maintained at 25 °C using a cellVivo microscope incubation system (Pecon GmbH, Germany).

Alginate Lyase Assay. We adapted a previously described agarose plate-based assay (44) to test the ability of monocultures and cocultures to secrete alginate lyases. For each strain, cultures were growth for 18 h in MB medium, and 1 mL of cell suspension was centrifuged (13,000 rpm for 2 min) in a 2-mL microfuge tube. The supernatant was discarded and the cell-pellet was subject to two rounds of washing with TR medium without any carbon source. The cell pellet was suspended in 1 mL of TR medium without carbon source and the optical density measured and adjusted to 0.1OD. For ZF270 monocultures 50 μL of 0.1OD culture, or for cocultures 50 μL of degrader and 50 μL of cross-feeder cultures, were mixed and spotted on plates that were made using TR medium containing 0.1% (w/v) alginate (Sigma Aldrich) and 1% agarose (Applichem). Colonies were allowed to grow for 36 h at 25 °C, and then, the plates were flooded with 2%. Gram's Iodine (Sigma Aldrich). The excess iodine was discarded and then imaged using an iPhone 12 camera. If cells secreted alginate lyases, then a distinct clearance zone was formed, the diameter of which was measured using a standard ruler. Before staining with iodine, the colonies were scraped and suspended in 200 μL of TR mediums (without carbon source) and subjected to 10-fold serial dilutions (until 10^{-5}). Cell numbers were measured for each condition by plating the dilutions on Marine Agar plates (DIFCO) and incubating for 30 h. ZF270 colonies (based on distinct morphology) were enumerated by manual counting on the plates.

Image Analysis. Cells within microscopy images were segmented using a custom-built Python-based (v3.7) segmentation workflow and tracked with SuperSegger (45). The output of segmentation and tracking were processed using Matlab v2017b or newer and R v4. Phase-contrast channel images were used for alignment following which fluorescence channel images were used for segmentation, tracking, and linking. Images were cropped at the boundaries of each microfluidic chamber. Growth properties and spatial locations were directly derived from the downstream processing tools of SuperSegger (gateTool and superSeggerViewer). Lineage trees, spatial distribution, and densities were computed using the x and y coordinates of cell over time. Spatial intercellular distances between ZF270 and cross-feeder cells were computed using the pcf and determining the intercellular distance where the pcf peaked in either coculture condition (https://physics.emory.edu/faculty/weeks/idl/gofr.html). Sections of code were written with the aid of ChatGPT-4.

Datasets and Statistical Analysis. All batch experiments were replicated 3 to 6 times. Growth curves were analyzed in Python v3.7 using the *Amiga* package

(46) and GraphPad Prism v8 (GraphPad Software, USA). The microscopy dataset set consists of eight, nine, and eight chambers, respectively for ZF270, ZF270+1F187, and ZF270 + A3M17. These are grouped into three biological replicates wherein each biological replicate is fed by media through a unique channel in a microfluidic chip. Cells with negative growth rates were excluded from the analysis after visual curation and represent artefacts, mistakes in linking during the segmentation or tracking process or nongrowing deformed cells. Each chamber was treated as an independent. Each figure depicts means or medians of all chambers for each condition. Pre-existing linear or exponential regression models from SciPy Stats v1.11.1 were applied in python v3.9 to determine relationships between independent measures. Comparisons were considered statistically significant when $P < 0.05$ or when false discovery rate (FDR) corrected $Q < 0.05$. FDR corrections were applied when multiple t tests were performed for the same dataset. Measures of effect size are represented by the R^2 or eta^2 value. All statistical analyses were performed in GraphPad Prism v 8.0 (GraphPad Software, USA), Rstudio v1.1.463 (Rstudio inc), and python v3.9. Plot formatting was unified in Adobe Illustrator v27.7.

Data, Materials, and Software Availability. All raw curated image analysis datasets, source data, and scripts are deposited in the ERIC and Zenodo repositories https://doi.org/10.5281/zenodo.8274002 (47).

Author affiliations: [a]Microbial Systems Ecology Group, Department of Environmental Systems Sciences, Institute of Biogeochemistry and Pollutant Dynamics, ETH-Zurich, Zurich 8006, Switzerland; [b]Department of Environmental Microbiology, Eawag: Swiss Federal Institute of Aquatic Sciences, Duebendorf 8600, Switzerland; [c]Department of Civil and Environmental Engineering, Massachusetts Institute of Technology, Cambridge, MA 02139; [d]Department of Civil, Environmental and Geomatic Engineering, Institute of Environmental Engineering, ETH Zurich, Zurich 8093, Switzerland; [e]Department of Marine Sciences, University of Georgia, Athens, GA 30602; and [f]Environmental Engineering Institute, School of Architecture, Civil and Environmental Engineering, École polytechnique fédérale de Lausanne, CH-1015 Lausanne, Switzerland

Author contributions: G.D., J.S., J.K., M.D., O.X.C., R.S., and M.A. designed research; G.D. performed research; J.S., J.E.S., M.D., O.X.C., and M.A. contributed new reagents/analytic tools; G.D. analyzed data; and G.D., J.S., J.K., J.E.S., R.S., and M.A. wrote the paper.

1. S. Pontrelli *et al.*, Metabolic cross-feeding structures the assembly of polysaccharide degrading communities. *Sci. Adv.* **8**, eabk3076 (2022).
2. J.-H. Hehemann *et al.*, Adaptive radiation by waves of gene transfer leads to fine-scale resource partitioning in marine microbes. *Nat. Commun.* **7**, 12860 (2016).
3. J. M. Grondin, K. Tamura, G. Déjean, D. W. Abbott, H. Brumer, Polysaccharide utilization loci: Fueling microbial communities. *J. Bacteriol.* **199**, e00860-16 (2017).
4. G. G. D'Souza, V. R. Povolo, J. M. Keegstra, R. Stocker, M. Ackermann, Nutrient complexity triggers transitions between solitary and colonial growth in bacterial populations. *ISME J.* **15**, 2614–2626 (2021), 10.1038/s41396-021-00953-7.
5. A. Dal Co, S. van Vliet, D. J. Kiviet, S. Schlegel, M. Ackermann, Short-range interactions govern the dynamics and functions of microbial communities. *Nat. Ecol. Evol.* **4**, 366–375 (2020).
6. K. Zengler, L. S. Zaramela, The social network of microorganisms–How auxotrophies shape complex communities. *Nat. Rev. Microbiol.* **16**, 383–390 (2018).
7. C. Arnosti *et al.*, The biogeochemistry of marine polysaccharides: Sources, inventories, and bacterial drivers of the carbohydrate cycle. *Ann. Rev. Mar. Sci.* **13**, 81–108 (2021).
8. A. Buchan, G. R. LeCleir, C. A. Gulvik, J. M. González, Master recyclers: Features and functions of bacteria associated with phytoplankton blooms. *Nat. Rev. Microbiol.* **12**, 686 (2014).
9. O. X. Cordero, M. S. Datta, Microbial interactions and community assembly at microscales. *Curr. Opin. Microbiol.* **31**, 227–234 (2016).
10. T. N. Enke *et al.*, Modular assembly of polysaccharide-degrading marine microbial communities. *Curr. Biol.* **29**, 1528–1535.e6 (2019).
11. G. D'Souza *et al.*, Ecology and evolution of metabolic cross-feeding interactions in bacteria. *Nat. Prod. Rep.* **35**, 455–488 (2018).
12. M. S. Datta, E. Sliwerska, J. Gore, M. F. Polz, O. X. Cordero, Microbial interactions lead to rapid micro-scale successions on model marine particles. *Nat. Commun.* **7**, 11965 (2016).
13. K. Amarnath *et al.*, Stress-induced metabolic exchanges between complementary bacterial types underly a dynamic mechanism of inter-species stress resistance. *Nat. Commun.* **14**, 3165 (2023).
14. A. Ebrahimi, J. Schwartzman, O. X. Cordero, Cooperation and spatial self-organization determine rate and efficiency of particulate organic matter degradation in marine bacteria. *Proc. Natl. Acad. Sci. U.S.A.* **116**, 23309–23316 (2019).
15. A. Ebrahimi, J. Schwartzman, O. X. Cordero, Multicellular behaviour enables cooperation in microbial cell aggregates. *Philos. Trans. R. Soc. B Biol. Sci.* **374**, 20190077 (2019).
16. J. A. Schwartzman *et al.*, Bacterial growth in multicellular aggregates leads to the emergence of complex life cycles. *Curr. Biol.* **32**, 3059–3069.e7 (2022), 10.1016/j.cub.2022.06.011.
17. G. D'Souza *et al.*, Cell aggregation is associated with enzyme secretion strategies in marine polysaccharide-degrading bacteria. *ISME J.* **17**, 703–711 (2023).
18. V. R. Povolo *et al.*, Extracellular appendages govern spatial dynamics and growth of *Caulobacter crescentus* on a prevalent biopolymer. bioRxiv [Preprint] (2022). https://doi.org/10.1101/2022.06.13.495907 (Accessed 13 June 2022).
19. K. Drescher, C. D. Nadell, H. A. Stone, N. S. Wingreen, B. L. Bassler, Solutions to the public goods dilemma in bacterial biofilms. *Curr. Biol.* **24**, 50–55 (2014).
20. H. Ertesvåg, Alginate-modifying enzymes: Biological roles and biotechnological uses. *Front. Microbiol.* **6**, 523 (2015).
21. A. K. M. Stubbusch *et al.*, Polysaccharide breakdown products drive degradation-dispersal cycles of foraging bacteria through changes in metabolism and motility. bioRxiv [Preprint] (2023). https://doi.org/10.1101/2023.07.14.548877 (Accessed 14 July 2023).
22. U. Alcolombri *et al.*, Sinking enhances the degradation of organic particles by marine bacteria. *Nat. Geosci.* **14**, 775–780 (2021).
23. Y. Yawata *et al.*, Competition-dispersal tradeoff ecologically differentiates recently speciated marine bacterioplankton populations. *Proc. Natl. Acad. Sci. U.S.A.* **111**, 5622–5627 (2014).
24. M. Daniels, S. van Vliet, M. Ackermann, Changes in interactions over ecological time scales influence single-cell growth dynamics in a metabolically coupled marine microbial community. *ISME J.* **17**, 406–416 (2023).
25. J. S. L. Yu *et al.*, Microbial communities form rich extracellular metabolomes that foster metabolic interactions and promote drug tolerance. *Nat. Microbiol.* **7**, 542–555 (2022).
26. Piccardi Philippe, Vessman Björn, Mitri Sara, Toxicity drives facilitation between 4 bacterial species. *Proc. Natl. Acad. Sci. U.S.A.* **116**, 15979–15984 (2019).
27. B. Schink, Energetics of syntrophic cooperation in methanogenic degradation. *Microbiol. Mol. Biol. Rev.* **61**, 262–280 (1997).
28. L. Oña *et al.*, Obligate cross-feeding expands the metabolic niche of bacteria. *Nat. Ecol. Evol.* **5**, 1224–1232 (2021).
29. S. Blasche *et al.*, Metabolic cooperation and spatiotemporal niche partitioning in a kefir microbial community. *Nat. Microbiol.* **6**, 196–208 (2021).
30. A. Dal Co, S. van Vliet, M. Ackermann, Emergent microscale gradients give rise to metabolic cross-feeding and antibiotic tolerance in clonal bacterial populations. *Philos. Trans. R. Soc. B Biol. Sci.* **374**, 20190080 (2019).
31. P. G. Egland, R. J. Palmer, P. E. Kolenbrander, Interspecies communication in *Streptococcus gordonii*-Veillonella atypica biofilms: Signaling in flow conditions requires juxtaposition. *Proc. Natl. Acad. Sci. U.S.A.* **101**, 16917–16922 (2004).
32. E. H. Wintermute, P. A. Silver, Dynamics in the mixed microbial concourse. *Genes Dev.* **24**, 2603–2614 (2010).
33. P. K. Singh *et al.*, *Vibrio cholerae* combines individual and collective sensing to trigger biofilm dispersal. *Curr. Biol.* **27**, 3359–3366.e7 (2017).
34. Y. J. Bomble *et al.*, Lignocellulose deconstruction in the biosphere. *Curr. Opin. Chem. Biol.* **41**, 61–70 (2017).
35. M. Ryan *et al.*, Interaction networks are driven by community-responsive phenotypes in a chitin-degrading consortium of soil microbes. *mSystems* **7**, e0037222 (2022).
36. M. J. McInerney, J. R. Sieber, R. P. Gunsalus, Syntrophy in anaerobic global carbon cycles. *Curr. Opin. Biotechnol.* **20**, 623–632 (2009).
37. M. J. McInerney *et al.*, The genome of Syntrophus aciditrophicus: Life at the thermodynamic limit of microbial growth. *Proc. Natl. Acad. Sci. U.S.A.* **104**, 7600–7605 (2007).
38. T. Bell, J. A. Newman, B. W. Silverman, S. L. Turner, A. K. Lilley, The contribution of species richness and composition to bacterial services. *Nature* **436**, 1157–1160 (2005).
39. M. Ackermann, A functional perspective on phenotypic heterogeneity in microorganisms. *Nat. Rev. Microbiol.* **13**, 497–508 (2015).
40. B. J. Tibbles, D. E. Rawlings, Characterization of nitrogen-fixing bacteria from a temperate saltmarsh lagoon, including isolates that produce ethane from acetylene. *Microb. Ecol.* **27**, 65–80 (1994).
41. G. D'Souza *et al.*, Less is more: Selective advantages can explain the prevalent loss of biosynthetic genes in bacteria. *Evolution* **68**, 2559–2570 (2014).
42. R. E. Lenski, M. R. Rose, S. C. Simpson, S. C. Tadler, Long-term experimental evolution in *Escherichia coli*. I. Adaptation and divergence during 2,000 generations. *Am. Nat.* **138**, 1315-1341 (1991).
43. R. Mathis, M. Ackermann, Response of single bacterial cells to stress gives rise to complex history dependence at the population level. *Proc. Natl. Acad. Sci. U.S.A.* **113**, 4224–4229 (2016).
44. S. S. Sawant, B. K. Salunke, B. S. Kim, A rapid, sensitive, simple plate assay for detection of microbial alginate lyase activity. *Enzyme Microb. Technol.* **77**, 8–13 (2015).
45. S. Stylianidou, C. Brennan, S. B. Nissen, N. J. Kuwada, P. A. Wiggins, SuperSegger: Robust image segmentation, analysis and lineage tracking of bacterial cells: Robust segmentation and analysis of bacteria. *Mol. Microbiol.* **102**, 690–700 (2016).
46. F. S. Midani, J. Collins, R. A. Britton, AMiGA: Software for automated analysis of microbial growth assays. *mSystems* **6**, e0050821 (2021).
47. G. D'Souza, Dataset for Interspecies interactions determine growth dynamics of biopolymer degrading populations in microbial communities. Zenodo. https://doi.org/10.5281/zenodo.8274002. Deposited 22 March 2023.